

Who Evaluates the Evaluations? Objectively Scoring Text-to-Image Prompt Coherence Metrics with T2IScoreScore (TS2)

Michael Saxon[✉] Fatima Jahara[✉] Mahsa Khoshnoodi[✉]
 Yujie Lu[✉] Aditya Sharma[✉] William Yang Wang[✉]
[✉]University of California, Santa Barbara [✉]Fatima Al-Fihri Predoctoral Fellowship
[✉]Equal contribution [✉]Contact: saxon@ucsb.edu
[T2IScoreScore.github.io](https://github.com/T2IScoreScore)

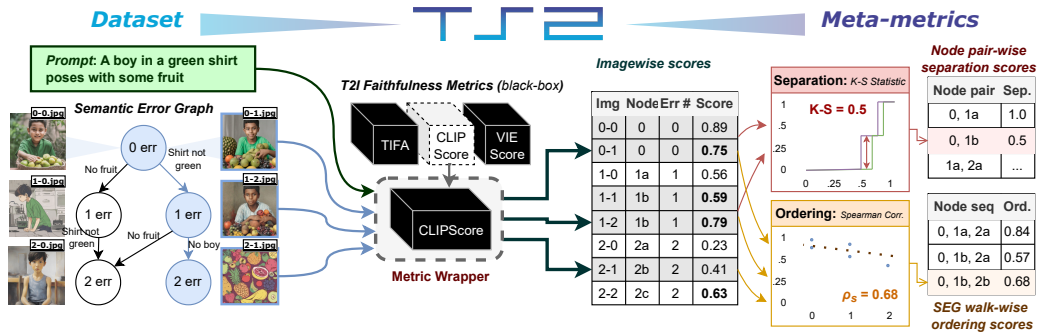


Figure 1: Overview of T2IScoreScore. T2I evaluation metrics are scored based on their ability to correctly organize images in a semantic error graph (SEG) relative to their generating prompt, checking ordering (Spearman’s ρ) and separation of nodes (Kolmogorov–Smirnov statistic).

Abstract

With advances in the quality of text-to-image (T2I) models has come interest in benchmarking their *prompt faithfulness*—the semantic coherence of generated images to the prompts they were conditioned on. A variety of T2I faithfulness metrics have been proposed, leveraging advances in cross-modal embeddings and vision-language models (VLMs). However, these metrics are not rigorously compared and benchmarked, instead presented with correlation to human Likert scores over a set of easy-to-discriminate images against seemingly weak baselines.

We introduce T2IScoreScore (TS2), a curated set of *semantic error graphs* containing a prompt and a set increasingly erroneous images. These allow us to rigorously judge whether a given prompt faithfulness metric can correctly order images with respect to their objective error count and significantly discriminate between different error nodes, using meta-metric scores derived from established statistical tests. Surprisingly, we find that the state-of-the-art VLM-based metrics (e.g., TIFA, DSG, LLMscore, VIEScore) we tested fail to significantly outperform simple (and supposedly worse) feature-based metrics like CLIPScore, particularly on a hard subset of naturally-occurring T2I model errors. TS2 will enable the development of better T2I prompt faithfulness metrics through more rigorous comparison of their conformity to expected orderings and separations under objective criteria.

1 Introduction

Text-to-image (T2I) models are improving at a breakneck pace in terms of quality, fidelity, and coherence of generated images to their conditioning prompts [1–4]. Despite this, persistent challenges in achieving image-prompt faithfulness [5, 6] remain—particularly in freely available models that don’t sit behind proprietary APIs. Indeed, many techniques to improve T2I models have been proposed of late, aiming to reduce hallucination [7, 8], duplication [9], composition errors [8, 10], and missing objects [11, 12]. However, there is no consensus on how to best compare these many models and methods, so it is hard to objectively track T2I progress [13, 14].

Recent work has proposed a litany of automated *image-prompt coherence metrics* which rate the *faithfulness* of generated images: the degree to which they satisfy the implicit requirements set forth in the generating prompt [15–18]. These proposed metrics vary considerably in design; as rating how well an image matches to its prompt is a nontrivial multimodal challenge [14, 19, 20].

This variety itself presents a *meta-evaluation problem*: there is no **consensus on how these faithfulness metrics ought to be compared**, and consequently each new metric is validated on its own ad-hoc test set against prior baselines. Typically these *self-evaluations* consist of a set of prompt-image pairs with accompanying human annotations (usually simple Likert scores [16, 19]), and metrics are judged on their correlation to these human judgements [20].

Such self-evaluation is not ideal; authors may unwittingly tilt the scales by using evaluation examples which cater to the particular strengths of their proposed method, and variance of metric performance between different evaluation sets (containing different images and prompt semantics [21, 22]) is high [23]. Additionally, relying on correlation to human judgements of small sets of images across different prompts is highly subjective [24, 25] and prone to including judgements of quality and style that are orthogonal to prompt coherence. We need a consistent and objective meta-evaluation.

To this end we propose **T2IScoreScore (TS2)**, a *benchmark and set of meta-metrics* for evaluating T2I faithfulness metrics. While it contains a similar number of images to previously proposed coherence metric evaluation sets, it contains fewer prompts. This high image-to-prompt ratio allows us to organize the images along *semantic error graphs*, or SEGs (fig. 1), where each edge corresponds to a specific error with respect to the prompt that a child image set possesses but its parent images do not. These semantic error graphs permit objective scoring of a metric by answering:

1. Can a metric correctly **order** increasingly wrong images against their generating prompt?
2. Can a metric reliably **separate** sets of images that differ by a specific semantic error?
3. Does the metric **confidently** separate the image sets within its dynamic range?

We adapt existing statistical tests [26, 27] to the SEG setting to answer these questions for a broad set of T2I faithfulness metrics. We find some surprising results: despite their inferior performance in correlating to human preferences against complicated vision-language model (VLM)-based metrics [6, 16–18], simple embedding-correlation methods like CLIPScore [15] are actually quite performant on our meta-metrics, and **Pareto-optimal** with respect to compute cost (§5). In summary, we:

- Formalize the task of objectively assessing T2I prompt coherence metrics by their ability to correctly order and separate image populations within semantic error graphs (SEGs). (§2)
- Present **T2IScoreScore (TS2)**, our evaluation for this task: a carefully-curated benchmark dataset of SEGs each containing between 4 and 76 images, permitting 93,000 total pairwise image comparisons and meta-metrics for ordering and separation in SEGs. (§2, §3)
- Evaluate a broad and representative set of T2I faithfulness benchmarks using **TS2**, demonstrate that it identifies novel failure cases, and motivate future work on improved metrics. (§4 §5, §6)

1.1 Related Work

Most evaluations in the T2I space test the quality of generating models based on *a fixed faithfulness metric’s scores over a fixed benchmark set of prompts*. Often these reference prompt sets are designed for testing a single specific capability. DrawBench [4], T2I-CompBench [28], and ABC-6k [8] focus on attributes like compositionality, cardinality, and spatial relations, in strictly text-guided image generation, while ImagenHub [14] tests them in a broader set of settings like image editing and subject-driven synthesis. Other evaluation dimensions such as multilinguality [29, 30] and stereotype bias [31] have also been explored. These prompts are usually sourced from some combination of

Dataset	# Images		Img. per Prompt		# Img Comparisons		Ad-hoc
	Total	T2I-Gen.	Avg	Per equiv. pref	Total	T2I Errors	
<i>Benchmarks for captioning models.</i>							
Flickr8k [32]	8k	0	0.2	0.2	8k	0	–
Flickr30k [33]	31k	0	0.2	0.2	31k	0	–
MSCOCO Captions [34]	330k	0	0.22	0.22	330k	0	–
<i>Benchmarks for image retrieval/matching models. (Could be used for T2I metric evaluation)</i>							
SeeTRUE [38]	31k	0	1	1	31k	0	✓
Pick-a-Pic [37]	500k	500k	2 ¹	1	7M	0	✓
<i>Benchmarks for T2I faithfulness metrics.</i>							
TIFA v1.0 [16]	800	800	5	1	4k	0	✓
DSG-1k [16]	1k	1k	1	1	1k	0	✓
T2IScoreScore	<i>2.8k</i>	<i>2690</i>	17	3.4	<i>93k</i>	3.1k	–

Table 1: Comparison of benchmark datasets that can be used to evaluate T2I faithfulness. *Per equiv pref* means the average number of images for each prompt that are assigned the same preference or correctness score. **Bold** numbers are best overall, *italic* are best of the T2I metric benchmarks.

existing natural image captioning resources [32–34] and sets of in-the-wild conditioning prompts produced by real users [35, 36]. These benchmarks assess image quality either by direct human analysis or automated metrics [14] including those we analyze in this work. Often the goal of these benchmarks is to analyze how well a model generates images that comport with human preferences [14, 37], and directly elicit opinions from users through a web interface for this purpose.

To meta-evaluate faithfulness metrics *a benchmark containing a fixed set of images and prompts is required*. However, all existing benchmarks for this purpose suffer from two key limitations:

1. Evaluating on noisy *human preference* rather than *explicitly labeled objective differences*
2. *Low image-to-prompt ratio* limiting evaluation of discriminatory power over similar images

Captioning benchmarks [32–34] are poor candidates for faithfulness metric evaluation as single images are paired with multiple prompt candidates rather than vice versa. Image matching and entailment benchmarks such as SeeTRUE [38] and Pick-a-Pic [37] are also limited by a low ratio.

The few extant deliberately-designed faithfulness evaluation sets are limited by both factors. TIFA v1.0 [16] and DSG-1k [6] were proposed *ad-hoc* to demonstrate the utility of their accompanying metrics by relating the scores assigned by the metric to human preferences. These are done over small sets of images (800 & 1000 respectively) with slightly more images-per-prompt (5 & 1).

The two limitations of these prior evals are linked. A reliance on human preference correlations is a natural consequence of having few and poorly organized images to compare to each prompt. A lack of meta-metrics designed for evaluating structured aspects other than human preference correlation means limited utility in collecting larger, structured sets of images for each prompt. By providing both *meta-metrics* **and** *a structured eval set* **T2IScoreScore** overcomes these limitations (table 1).

2 T2IScoreScore meta-metrics

We introduce three measures of ordering and separation by a given metric within semantic error graphs (SEGs). We define SEG S as prompt P and a directed acyclic graph of nodes n_i containing one or more images I_j sharing the same errors wrt. the prompt. We label each node by its error count and type (eg, [0, 1a, 1b] has 1 node with 0 errors, and 2 nodes with 1 error each of different type).

A good prompt coherence metric will correctly rank images along each walk of increasing error counts within a SEG, and separate the scores assigned to images in successive nodes. Our metrics assess this by evaluating each walk separately. For ease of notation, we refer to each SEG as a set of walks $W \in S$ over nodes of increasing error count (eg, (0, 1a, 2a), (0, 1a, 2b), etc), where each walk is the in-order set of all (image, prompt, num. error) triples $(I, P, N) \in W$. For example, the first walk in fig. 1 is [(0-0 . jpg, P , 0), (0-1 . jpg, P , 0), (1-0 . jpg, P , 1), (2-0 . jpg, P , 2), ...].

We introduce measures of metric m for SEG S : $\text{rank}_m(S)$, $\text{sep}_m(S)$ & $\text{delta}_m(S)$, assessed over every walk $W \in S$ in all SEGs in the **TS2** dataset to score a metric. They’re defined as:

¹Although this benchmark has 14 pairs of images per prompt, each pair is separately annotated. With no way to compare between pairs, the effective number of images per prompt is 2, with many repeated prompts.

2.1 Ordering score over walks: rank_m

We use Spearman’s rank correlation coefficient ρ [26] between image-level error count and metric-assigned score over every walk on a SEG to assess how a metric’s faithfulness score aligns to our objective structure error counts. Spearman’s ρ is the PCC of the rank order of variables X, Y :

$$\rho(X, Y) = \frac{\text{cov}(R(X), R(Y))}{\sigma_{R(X)}\sigma_{R(Y)}}; \quad R(X) = \left\{ \sum_{x_i \in X} \mathbb{1}(x_i < x) \mid x_i \in X \right\} \quad (1)$$

Thus, in our case the SEG-level rank order score $\text{rank}_m(S)$ for scoring model m is defined as:

$$\text{rank}_m(S) = \frac{1}{|S|} \sum_{W \in S} r_s(\{m(I, P) \mid (I, P, N) \in W\}, \{N \mid (I, P, N) \in W\}) \quad (2)$$

One limitation of Spearman’s ρ for characterizing scores is that it is undefined if one set $R(U)$ exclusively contains identical elements, as $\sigma_{R(U)} = 0$. For tractability in these scenarios we define $\rho(\cdot, R(U)) := 0$, in these cases. If a metric assigns identical scores to all examples across different error levels, it presents no discernible relationship between error severity and score for that image set.

2.2 Statistical separation of error populations score: sep_m

We assess the two-sample Kolmogorov–Smirnov statistic [27] pairwise between the populations of metric m ’s scores assigned to each sample between two error nodes n_i and n_j as populations. The Kolmogorov–Smirnov statistic is a non-parametric measure of the separation between two distributions [39, 40], defined as the maximum vertical difference between their empirical cumulative distribution functions $F_X(s)$:

$$D_{KS}(X, Y) = \sup_{x \in R_m} |F_X(x) - F_Y(x)| \quad (3)$$

Where $F_X(x)$ is proportion of samples in population X for which the metric-assigned score $m(i) \leq x$, (see fig. 8 for a visual depiction). We compute D_{KS} for every pair of adjacent error nodes in each tree walk W^2 , and report the average over all of these as the SEG separation score $\text{sep}_m(S)$:

$$\text{sep}_m(S) = \frac{1}{|S|} \sum_{n_i \in S} D_{KS}(\{m(P, I) \mid (P, I) \in n_i\}, \{m(P, I) \mid (P, I) \in n_{i+1}\}) \quad (4)$$

2.3 Separation of nodes within dynamic range: delta_m

While sep_m nonparametrically estimates whether pairs of nodes are drawn from different distributions (and thereby distinguished), it provides no information about the distance by which they are separated within the metric’s dynamic range. This measure gives an alternative look at separation between nodes: the more separation a metric provides between nodes, the less severe slight variations in assigned score will be to ignoring errors in generated images. We assess it as:

$$\text{delta}_m(S) = \frac{1}{|S|\sigma_{m(\forall S)}} \sum_{N_i \in W} \text{avg}(\{m(P, I) \mid (P, I) \in N_i\}) - \text{avg}(\{m(P, I) \mid (P, I) \in N_{i+1}\}) \quad (5)$$

Where $\sigma_{m(\forall S)}$ is the standard deviation of scores from metric m on all images in all SEGs in **TS2**. Our score is the average distance between the mean metric score of all adjacent nodes in all SEGs, rescaled by the standard deviation of the score to normalize against the metric’s dynamic range.

3 The **T2IScoreScore** Dataset

We now turn to describing the **TS2** dataset collection process. We use three different semantic error graph collection procedures to produce a diverse set of SEGs. Each contains one prompt and between 4 and 76 images assigned to error nodes. Each node usually contains more than one image, though for simplicity in presentation we only show one image assigned to each node in this section.

²We use individual nodes $n_i \in S$ containing pairs of prompt, image $(P, I) \in n_i$ to make this equation easier to read.

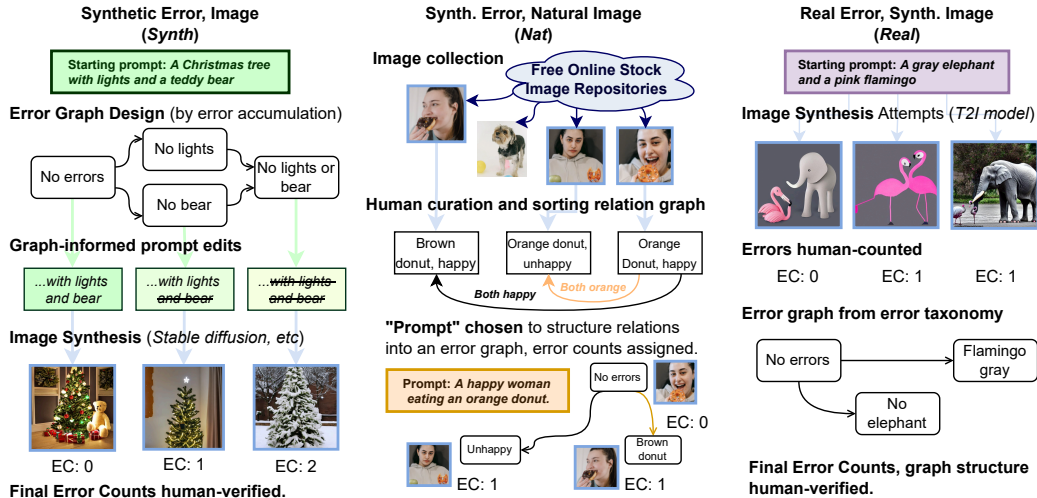


Figure 2: The three *semantic error graphs* production procedures. **Synth.** (images generated from multiple prompts written to populate a SEG), **Nat.** (natural images populate a SEG), and **Real** (real errors from image generation attempts from one prompt populate a SEG).

3.1 Dataset Collection Procedure

Figure 2 depicts the three procedures by which we produce and populate SEGs with images: **synthetic** images from a synthetic graph (*Synth*), graph from **natural** images (*Nat*), and graph from **real** errors of synthetic images (*Real*), differentiated by prompt source, image source, and the order of production.

Synth. Synthetic SEGs are produced “graph first.” From an initial prompt, we construct an error graph by first listing all entities and properties prescribed in the prompt, and then ablating them to produce the nodes, for which writing prompts without those elements to generate their images. For example, in the left panel of fig. 2, from the initial prompt “a Christmas tree with lights and a teddy bear” prompts containing errors such as “a Christmas tree with lights” are produced. We generate images using a T2I models (listed in §3.2) for each prompt and verify node-image faithfulness.

Nat. The natural error trees exclusively contain real images sourced from the free stock image repository *Pexels*. We generate SEGs in “image, graph, prompt” order. We source sets of natural images that share objects and models. We organize them by relation graphs describing how the images differ by objects, actions, attributes, and composition. We then select a head node in this relation graph and write a “prompt” describing this head node (eg., fig. 2 center panel). We produced SEGs of natural images to assess whether distributional differences between synthetic images and real images might lead to measurable impacts on performance for the faithfulness metrics that typically use base models pretrained exclusively on natural images [41].

Real. The real error, synthetic image examples are following a “prompt, image, graph” order of production. We simply generate a large set of images using a T2I model with a single prompt, annotate the errors in each generated image to produce the error graph for the final SEG. This procedure is documented in the right panel of fig. 2.

3.2 Dataset structure, size, and validity

Each of the 165 SEGs in **TS2** is manually checked by three human annotators. The head node of each SEG contains at least one image that has been assessed by the annotators to contain no errors of verbal information (eg, entity in the image isn’t performing the described action), compositionality (eg, object described as “on top” but is beneath object), missing objects, or incorrect object attributes.

Each edge on the SEG represents an error of one of the aforementioned types. Each node is labeled with the number of edges along its shortest path back to node 0, representing its error count (fig. 1, fig. 8). Each node contains at least one image which is erroneous according to the described errors.

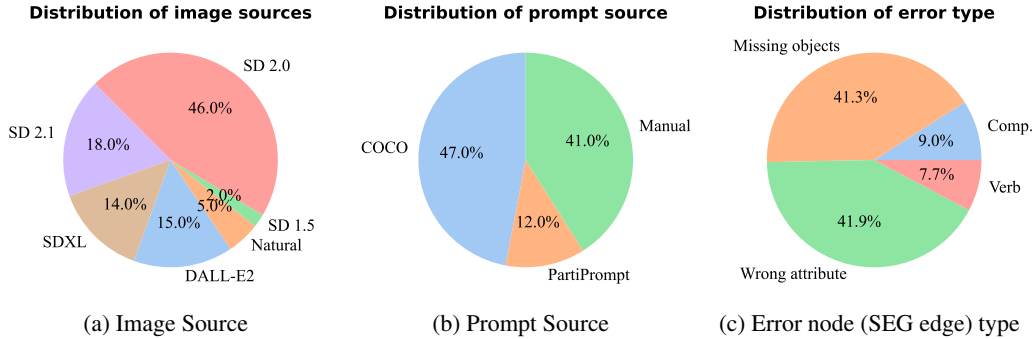


Figure 3: Overview of the distribution of sample types in **TS2**: (a) Where source images came from: 5% of images in the benchmark are real photographs from Pexels, while the remainder were generated by Stable Diffusion (SD) or DALL-E variants. (b) Source of the eliciting prompt; either existing resources or us (Manual). (c) Distribution of error types edges in all SEGs.

The synthetic images are generated with several T2I models—including DALL-E 2 [2], Stable Diffusion 1.5 [3], 2.0, 2.1, and SDXL [42]. We use MS-COCO [43], PartiPrompt [35], and manually written prompts in head nodes for the Synth and Real subsets. Image sources, prompt sources, and error type statistics are documented in fig. 3.

The total number of images and prompts is roughly in line with previous benchmarks that have been used to verify methods such as TIFA [16] and DSG [6] in their own papers, and permits significantly more image comparisons-per-prompt than any prior benchmark (Table 1), which we submit is the primary type of comparison required to verify that prompt-faithfulness assessments work.

4 Experiments

Using **TS2** we evaluated three classes of T2I evaluation metrics: *embedding-correlation* (comparing embeddings of prompt and image), *QG/A* (using VQA to check if requirement questions generated from the prompt are satisfied) and *caption-based* (comparing captions extracted from the generated images to the prompt). We evaluate these metrics with multiple backend VLMs (§A.2).

For each metric, we score every image against its SEG’s prompt. We report the results of our Ordering and Separation metrics across all SEGs, as well as for our the Synth, Nat, and Real SEG subsets.

4.1 Embedding-correlation Metrics

CLIPScore [15] is a popular prompt faithfulness metric based on simple text-image similarity. CLIPScore is computed as the cosine similarity of the L_2 -normalized CLIP-assessed [41] image and text embeddings. Equations and details in §A.1.

ALIGNScore (not to be confused with the text-only *AlignScore* [44]) is a variant embedding-based similarity score we produced using the ALIGN [45] embedding model rather than CLIP to embed the prompt and image. Other than model it is equivalent to CLIPScore.

4.2 Question Generation & Answering (QG/A) Metrics

Question Generation & Answering Metrics use an LM \mathcal{M}_{QG} to produce a set of requirement question/answer pairs $(q, a) \in Q$ from prompt p , and then use a vision-language model \mathcal{M}_{VL} to check each requirements against the image, reporting satisfaction rate as the image’s faithfulness score. QG/A metrics vary by how questions are generated and relate to each other. Equations in §A.1.

TIFA [16] prompts an LM (GPT-3) to generate a set of multiple choice and yes-no questions and their expected answers relative to the prompt. Then a vision language model \mathcal{M}_{VL} produces “free-form” answers to each question, which are converted into multiple choice answers a' using an SBERT model. The TIFA score for a given image is then the rate of correct answers.

		CLIPScore	ALIGNScore	mPLUG	LLaVA 1.5	LLaVA 1.5 (alt)	InstructBLIP	BLIP1	Fuyu	GPT4V	mPLUG	LLaVA 1.5	LLaVA 1.5 (alt)	InstructBLIP	BLIP1	Fuyu	GPT4V	LLMScore EC	LLMScore Over	VIEScore
		Emb-based			TIFA					DSG					Caption-based					
rank _m	Avg	71.4	73.9	71.0	74.5	74.4	76.5	73.8	38.7	77.9	70.4	76.2	75.0	79.0	76.6	29.5	79.6	48.8	57.7	37.8
	Synth	75.0	77.6	72.6	79.2	79.2	80.2	78.8	44.5	83.6	74.6	80.1	81.6	85.1	81.6	35.4	82.6	50.2	61.6	42.5
	Nat	58.0	70.2	66.9	62.8	64.0	65.1	62.2	23.5	61.6	65.3	65.9	68.8	70.7	71.6	20.5	73.7	36.2	44.4	22.4
	Real	69.3	62.6	68.2	66.7	64.5	71.6	64.0	29.7	69.5	58.4	70.0	54.2	62.0	61.2	14.2	73.0	54.4	54.1	33.2
sep _m	Avg	90.7	92.8	80.6	82.5	81.9	85.0	81.8	67.2	83.2	78.4	83.1	80.3	84.2	80.8	63.6	84.2	73.6	73.5	51.8
	Synth	90.5	94.1	80.6	85.5	85.2	86.7	84.1	67.3	86.2	80.9	85.7	83.9	87.8	84.9	65.8	86.6	71.1	72.8	53.7
	Nat	91.5	92.6	84.2	75.1	75.6	82.8	77.9	75.7	80.5	71.2	80.9	76.7	81.8	73.3	68.6	81.7	80.5	76.7	44.5
	Real	90.3	87.9	77.4	76.8	74.4	80.5	76.4	59.3	73.7	75.1	74.5	69.4	71.9	70.8	50.3	76.6	77.3	73.6	50.7
delta _m	Avg	89.7	95.6	92.4	97.5	97.1	99.8	94.0	43.9	92.3	94.2	104.7	102.0	110.6	103.7	37.7	110.2	66.9	56.3	45.9
	Synth	89.9	95.6	92.5	97.6	97.3	99.9	93.9	44.6	92.5	94.4	104.7	102.1	110.7	103.6	37.8	110.1	67.2	56.7	46.7
	Nat	92.5	98.6	94.4	98.7	98.8	101.1	95.5	46.1	93.9	96.0	105.5	103.0	111.6	104.6	39.3	111.5	66.2	56.4	46.6
	Real	95.1	100.8	96.0	100.5	100.4	102.6	96.9	46.9	95.9	97.3	106.8	104.2	113.0	105.9	39.4	113.0	65.0	56.0	46.3
Est. FLOP/run		604N	688M	224T	224T	224T	224T	224T	224T	1.66P	140T	140T	140T	140T	140T	140T	860T	7.01T	7.01T	2.6P

Table 2: Spearman ordering score rank_m, and Kolmogorov–Smirnov separation score sep_m, average dynamic range delta delta_m, (all reported as % for readability) and estimated FLOPs to score an image for each model. Best **bold**, within 2% of best *italic*, top four colored by metric type (emb-based, TIFA, DSG, caption-based). See §A.3 for information on how we estimate compute costs.

DSG (*Davidsonian scene graph*) [6] shares the QA structure of TIFA, but generates a set of requirement questions which are non-overlapping, have exclusively yes/no answers, and sit on a directed acyclic graph such that a question is only satisfied if it and all its parent questions are answered yes.

Backend VLMs. All QG/A metrics rely on the use of a generative vision-language model (VLM) either for performing question answering (\mathcal{M}_{VL} in §4.2) or captioning (\mathcal{M}_C in §4.3). Thanks to the simple decomposable framework of the QG/A methodologies, we were able to efficiently test the performance of both TIFA and DSG using several VLMs as visual question-answering backends $MVL\mathcal{M}_{VL}$. We used mPLUG, LLaVA, BLIP, InstructBLIP, Fuyu, and GPT-4V as VLM backends for the QG/A metrics. Details and reference for each VLM is provided in appendix §A.2.

4.3 Caption-comparison Metrics

LLMScore [17] captures the fine-grained similarity between the image and text with rationales by leveraging the visual details understanding capability from vision experts and the reasoning capability of LLMs. The visual information is parsed in hierarchical scene descriptions with global and local captions. Then the text-only LLM (we use GPT3) will compare the multi-granularity visual descriptions with the input text prompt to give a score according to the evaluation guideline prompt.

VIEScore [18] rates aspects of semantic consistency (SC) and perceptual quality (PQ) ultimately providing a rating score on a scale of 0 and 10. We use 0-shot LLaVA-1.5 as the backbone MLLM to evaluate how successfully the image follows the text-to-image prompt.

5 Results

Table 2 shows the results for the **Ordering** feature rank_m and **Separation** features sep_m and delta_m for each metric we assessed, on average for all SEGs (Avg), and the three SEG subsets, as well as an approximate FLOP cost per run for each metric (§A.3).

We found that the Synth set consisting of hand-designed (and probably more obvious) errors was the easiest subset for all metrics to correctly order. The average rank_m score for Synth across all metrics was 70%, for Nat 55% and for Real 56%. However, different subsets were hard for different classes of metrics. For the QG/A metrics, Real was hardest, while Nat was harder for the other classes.

As the embedding-correlation metrics came first, TIFA [16], DSG [6], LLMScore [17], and VIEScore [18] all compare themselves against a CLIPScore baseline [15]. Despite the superiority these metrics supposedly held on their respective ad-hoc evaluations, *the computationally cheaper CLIPScore and ALIGNScore are Pareto-optimal in most cases* (Figure 4), sharing the optimality frontier with DSG or TIFA with GPT-4V, methods that are ≈ 6 orders of magnitude more computationally expensive.

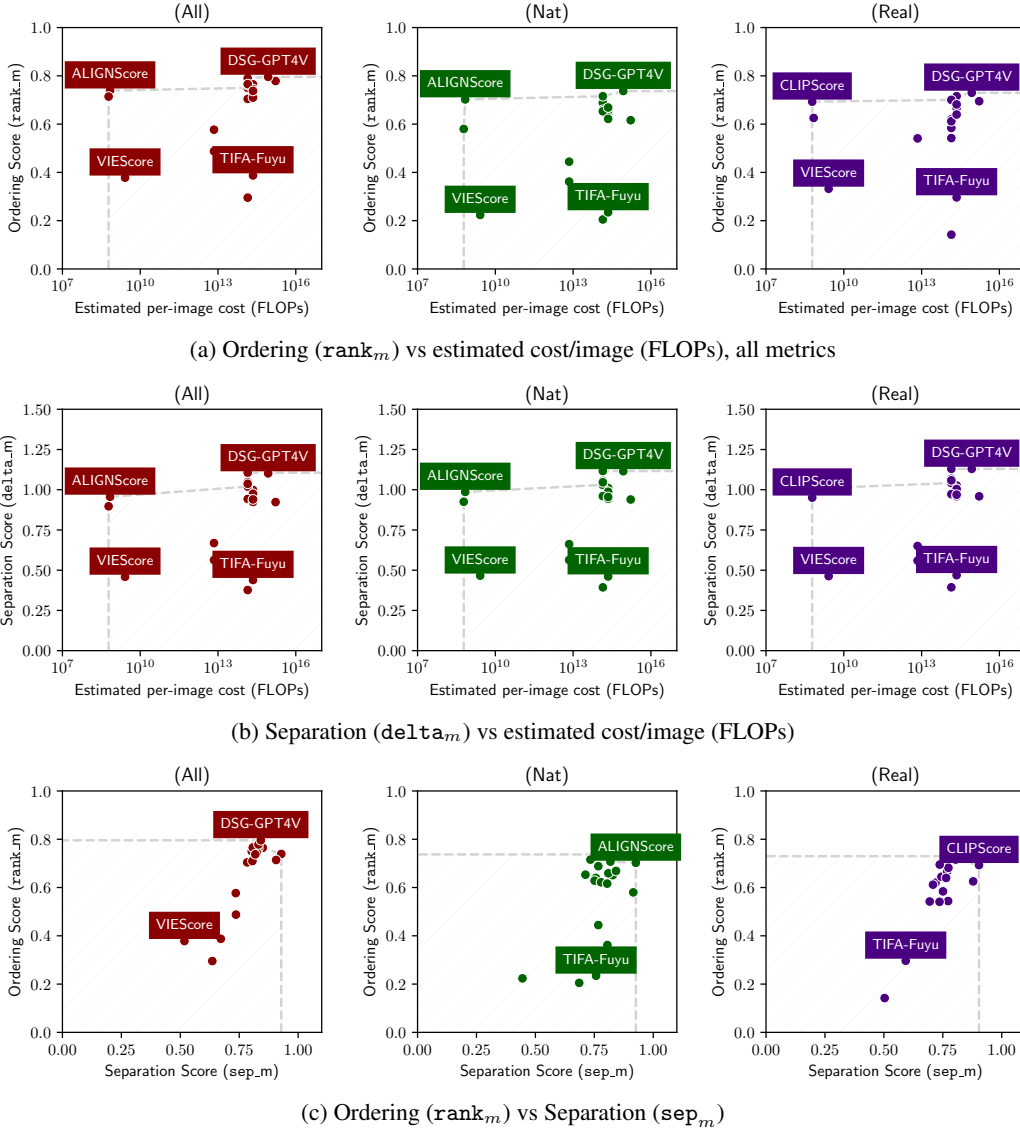


Figure 4: Plots of ordering and separation scores against estimated per-image metric evaluation costs in FLOPs and each other. For all analyses, the Pareto optimal metrics are DSG and TIFA with GPT-4, and the vastly less expensive embedding-correlation ALIGNScore and CLIPScore.

6 Discussion

The headline takeaway from our findings is that, contrary to claims of superiority leveled in their own papers, for all the QG/A and caption-comparison metrics [6, 16–18], *the cheap embedding-correlation metrics such as CLIPScore are sufficient or even preferable* at capturing objective semantic errors relative to fixed prompts. We view this capacity to accurately discriminate similar images relative to a prompt as the core feature a good prompt faithfulness metric must possess.

Why do we care about compute cost? When evaluating T2I models at release, compute costs are not very important—an evaluation only has to be run on a small set of images from benchmark prompts.

However, during training or in online monitoring, compute cost for faithfulness metrics becomes quite important. Faithfulness metrics could be used as reward signals while training a T2I model (or prompt generator), or called repeatedly during validation passes. Faithfulness metrics could be deployed in applications to guide an online prompt refinement system, to trigger a second call in user-facing applications, or to analyze prompt corpora to surface challenging examples for further

training or analysis. In all of these settings, a performant, low-cost model such as CLIPScore is valuable. **TS2** demonstrates that the performance premium for the expensive metrics is quite small.

Some desirable attributes in T2I metrics are not captured by **T2IScoreScore**. Human aesthetic preferences are—by design—ignored in **TS2** meta-evaluation. Though the QG/A and caption-comparison metrics fail to meaningfully outperform the cheap embedding-correlation metrics, they may have advantages that are not captured by **TS2**, such as in modeling human aesthetic preferences. Paired with a standalone benchmark of human aesthetic preferences over error-free images, a metric’s error assessment and aesthetic fidelity could be measured independently.

As the first objective evaluation of faithfulness metrics based on structural semantic errors, **TS2** enables more fine-grained measurement of metric desiderata, leading researchers to build better metrics, and empowering developers to make tradeoff-informed metric choices.

6.1 Systematic advantages for some metrics

One disadvantage of using Spearman’s ρ is that it “expects” ties to be the same in both distributions. For example, if a set of images has error count $(0, 1, 1, 2)$, the ordering $(1, 0.5, 0.5, 0)$ will have a perfect $\rho = 1$, while the ordering $(1, 0.51, 0.49, 0)$ will be penalized, despite it also presenting a correct ordering. This means that **our Ordering score** rank_m **systematically punishes the embedding-based metrics relative to the VLM-based ones**, as the embedding-correlation metrics CLIPScore and ALIGNScore can take continuous values, while TIFA, DSG, LLMScore, and VIEScore have a discrete range. In light of this systematic disadvantage for embedding-correlation metrics, it is even more striking that CLIP/ALIGNScore still are so performant and on the optimality frontier.

6.2 Near-perfect performance on rank_m and sep_m possible

Although the scores of many models on our metric are high, this meta-evaluation is far from “solved.” In principle it should be possible to get much closer to 100 on average for both meta-metrics than we find. We view use of **TS2** as a necessary secondary evaluation for any new proposed T2I faithfulness metric; if it has high correlation to subjective human judgements but does not perform well on **T2IScoreScore**, skepticism might be warranted.

6.3 Impact of future VLM advances

Ultimately, all image coherence evaluation metrics stand to improve from further advances in general VLM quality. As a considerably more performant model than LLaVA, mPLUG, etc, it was unsurprising that GPT4-V worked much better as a backbone for TIFA and DSG than the aforementioned. However, there do appear to be diminishing returns, as the order of magnitude going from mPLUG- to GPT4-V-based evaluation yielded a sub-1% improvement in rank_m performance on the most difficult and construct-valid Real set. Better constraint-generating processes may be required to push VLM-based evaluation metrics further.

7 Conclusion

We introduced **T2IScoreScore**, a first-of-its kind objective evaluation for text-to-image faithfulness metrics that utilizes a high image-to-prompt ratio to organize its reference images along semantic error graphs, through which a faithfulness metric can be assessed by our novel graph-based meta-metrics. Our study reveals a surprising finding: more expensive and recent “state of the art” VLM-metrics actually only have modest gains in performance over simpler and cheaper embedding-based metrics at best. Indeed, these cheap metrics such as CLIPScore and ALIGNScore are actually Pareto optimal along with the vastly more expensive and slightly more performant GPT-4V-based QG/A metrics, even when strictly comparing ordering and separation capabilities (leaving compute cost aside).

This underscores the necessity for a more nuanced approach to benchmarking and developing metrics capable of capturing the subtle semantic nuances between prompts and generated images. The establishment of **T2IScoreScore** as a benchmarking tool is a significant step forward, offering a structured way to rigorously test and improve T2I prompt faithfulness metrics, ensuring they can more accurately reflect the semantic coherence between prompts and generated images, thereby facilitating the development of more reliable and effective T2I models.

Limitations, ethical considerations, and impact

Limitations to our work are discussed throughout. For example, in §6.1 we discuss how our meta-metrics are limited by intrinsic biases of rank-correlation metrics among ties (many of which occur when multiple images occupy one node on a SEG). Additionally, compared to other evaluation sets, our total number of prompts is modest (this is required to achieve a high image-to-prompt ratio, however, which is a core strength of our work). Finally, due to its secretive nature, we are only able to produce *rough estimates of the compute cost of GPT-3 and GPT-4 based metrics*. We estimate them to the best of our ability using third-party information (§A.3).

This research will steer the development of more effective faithfulness metrics, which in turn will guide T2I model development. T2I models are inherently dual-use: they can be used to produce misinformation and other harmful content in addition to useful and entertaining imagery. Any work that contributes to improving their overall performance necessarily drives a small amount of both positive and deleterious impact in this way.

Acknowledgements

We thank the organizers and sponsors of the Fatima Al-Fihri Predoctoral Fellowship program for compute resources. This work was supported in part by the National Science Foundation Graduate Research Fellowship under Grant No. 1650114, and CAREER Award under Grant No. 2048122.

Contribution Statement

MS checked SEGs, designed the benchmark and meta-metrics, implemented the SEG tree iteration process and evaluation code for the ordering and separation scores, collated the QG/A answers into ID-level scores, and assessed the final scores.

MK produced the Nat SEGs and produced, annotated, and checked the other SEGs. MK generated the TIFA and DSG questions for all prompts, implemented and evaluated CLIPScore and ALIGNScore, collected answers for the QG/A metrics from BLIP, InstructBLIP, GPT-4V and refactored code.

FJ produced and annotated the Synth SEGs, produced and annotated a subset of the Real SEGs, and checked all others. FJ collected answers for Fuyu for the QG/A metrics and cleaned and organized the final dataset release.

YL evaluated LLMscore for the examples and conceived of measuring faithfulness errors in T2I faithfulness metrics. AS collected answers for the QG/A metrics from LLaVA and VIEScore.

References

- [1] Aditya Ramesh, Mikhail Pavlov, Gabriel Goh, Scott Gray, Chelsea Voss, Alec Radford, Mark Chen, and Ilya Sutskever. Zero-shot text-to-image generation. In *International Conference on Machine Learning*, pages 8821–8831. PMLR, 2021. 2
- [2] Aditya Ramesh, Prafulla Dhariwal, Alex Nichol, Casey Chu, and Mark Chen. Hierarchical text-conditional image generation with clip latents, 2022. 6
- [3] Robin Rombach, Andreas Blattmann, Dominik Lorenz, Patrick Esser, and Björn Ommer. High-resolution image synthesis with latent diffusion models. In *Proceedings of the IEEE/CVF Conference on Computer Vision and Pattern Recognition (CVPR)*, pages 10684–10695, June 2022. 6
- [4] Chitwan Saharia, William Chan, Saurabh Saxena, Lala Li, Jay Whang, Emily L Denton, Kamyar Ghasemipour, Raphael Gontijo Lopes, Burcu Karagol Ayan, Tim Salimans, et al. Photorealistic text-to-image diffusion models with deep language understanding. *Advances in Neural Information Processing Systems*, 35:36479–36494, 2022. 2
- [5] Vitali Petsiuk, Alexander E Siemenn, Saisamrit Surbehera, Zad Chin, Keith Tyser, Gregory Hunter, Arvind Raghavan, Yann Hicke, Bryan A Plummer, Ori Kerret, et al. Human evaluation of text-to-image models on a multi-task benchmark. *arXiv preprint arXiv:2211.12112*, 2022. 2

- [6] Jaemin Cho, Yushi Hu, Roopal Garg, Peter Anderson, Ranjay Krishna, Jason Baldridge, Mohit Bansal, Jordi Pont-Tuset, and Su Wang. Davidsonian scene graph: Improving reliability in fine-grained evaluation for text-to-image generation, 2024. 2, 3, 6, 7, 8, 16, 17, 21
- [7] Shengqiong Wu, Hao Fei, Hanwang Zhang, and Tat-Seng Chua. Imagine that! abstract-to-intricate text-to-image synthesis with scene graph hallucination diffusion. *Advances in Neural Information Processing Systems*, 36, 2024. 2
- [8] Weixi Feng, Xuehai He, Tsu-Jui Fu, Varun Jampani, Arjun Akula, Pradyumna Narayana, Sugato Basu, Xin Eric Wang, and William Yang Wang. Training-free structured diffusion guidance for compositional text-to-image synthesis. *arXiv preprint arXiv:2212.05032*, 2022. 2
- [9] Long Lian, Boyi Li, Adam Yala, and Trevor Darrell. Llm-grounded diffusion: Enhancing prompt understanding of text-to-image diffusion models with large language models. *arXiv preprint arXiv:2305.13655*, 2023. 2
- [10] Nan Liu, Shuang Li, Yilun Du, Antonio Torralba, and Joshua B Tenenbaum. Compositional visual generation with composable diffusion models. In *European Conference on Computer Vision*, pages 423–439. Springer, 2022. 2
- [11] Jezia Zakraoui, Moutaz Saleh, Somaya Al-Maadeed, and Jihad Mohammed Jaam. Improving text-to-image generation with object layout guidance. *Multimedia Tools and Applications*, 80(18):27423–27443, 2021. 2
- [12] Weixi Feng, Wanrong Zhu, Tsu-jui Fu, Varun Jampani, Arjun Akula, Xuehai He, Sugato Basu, Xin Eric Wang, and William Yang Wang. Layoutgpt: Compositional visual planning and generation with large language models. *Advances in Neural Information Processing Systems*, 36, 2024. 2
- [13] Tim Salimans, Ian Goodfellow, Wojciech Zaremba, Vicki Cheung, Alec Radford, and Xi Chen. Improved techniques for training gans. *Advances in neural information processing systems*, 29, 2016. 2
- [14] Max Ku, Tianle Li, Kai Zhang, Yujie Lu, Xingyu Fu, Wenwen Zhuang, and Wenhui Chen. Imagenhub: Standardizing the evaluation of conditional image generation models, 2023. 2, 3
- [15] Jack Hessel, Ari Holtzman, Maxwell Forbes, Ronan Le Bras, and Yejin Choi. Clipscore: A reference-free evaluation metric for image captioning. In *Proceedings of the 2021 Conference on Empirical Methods in Natural Language Processing*, pages 7514–7528, 2021. 2, 6, 7
- [16] Yushi Hu, Benlin Liu, Jungo Kasai, Yizhong Wang, Mari Ostendorf, Ranjay Krishna, and Noah A. Smith. TIFA: Accurate and Interpretable Text-to-Image Faithfulness Evaluation with Question Answering. URL <http://arxiv.org/abs/2303.11897>. 2, 3, 6, 7, 8, 16, 21
- [17] Yujie Lu, Xianjun Yang, Xiujun Li, Xin Eric Wang, and William Yang Wang. Llm-score: Unveiling the power of large language models in text-to-image synthesis evaluation. *arXiv preprint arXiv:2305.11116*, 2023. 7
- [18] Max Ku, Dongfu Jiang, Cong Wei, Xiang Yue, and Wenhui Chen. Viescore: Towards explainable metrics for conditional image synthesis evaluation. *arXiv preprint arXiv:2312.14867*, 2023. 2, 7, 8, 21
- [19] Emily L Denton, Soumith Chintala, Rob Fergus, et al. Deep generative image models using a laplacian pyramid of adversarial networks. *Advances in neural information processing systems*, 28, 2015. 2
- [20] Kimin Lee, Hao Liu, Moonkyung Ryu, Olivia Watkins, Yuqing Du, Craig Boutilier, Pieter Abbeel, Mohammad Ghavamzadeh, and Shixiang Shane Gu. Aligning text-to-image models using human feedback. *arXiv preprint arXiv:2302.12192*, 2023. 2
- [21] Michael Saxon, Xinyi Wang, Wenda Xu, and William Yang Wang. Peco: Examining single sentence label leakage in natural language inference datasets through progressive evaluation of cluster outliers. In *Proceedings of the 17th Conference of the European Chapter of the Association for Computational Linguistics*, pages 3053–3066, 2023. 2
- [22] Joseph P McKenna, Samridhi Choudhary, Michael Saxon, Grant P Strimel, and Athanasios Mouchtaris. Semantic complexity in end-to-end spoken language understanding. *arXiv preprint arXiv:2008.02858*, 2020. 2

- [23] Wanrong Zhu, Xin Eric Wang, Pradyumna Narayana, Kazoo Sone, Sugato Basu, and William Yang Wang. Towards understanding sample variance in visually grounded language generation: Evaluations and observations. *arXiv preprint arXiv:2010.03644*, 2020. 2
- [24] Phillip Isola, Jun-Yan Zhu, Tinghui Zhou, and Alexei A Efros. Image-to-image translation with conditional adversarial networks. In *Proceedings of the IEEE conference on computer vision and pattern recognition*, pages 1125–1134, 2017. 2
- [25] Chenlin Meng, Yutong He, Yang Song, Jiaming Song, Jiajun Wu, Jun-Yan Zhu, and Stefano Ermon. Sdedit: Guided image synthesis and editing with stochastic differential equations. *arXiv preprint arXiv:2108.01073*, 2021. 2
- [26] Charles Spearman. The proof and measurement of association between two things. *The American Journal of Psychology*, 15(1):72–101, 1904. ISSN 00029556. URL <http://www.jstor.org/stable/1412159>. 2, 4
- [27] Andrey Nikolaevich Kolmogorov. Sulla determinazione empirica di una legge didistribuzione. *Giorn Dell’inst Ital Degli Att*, 4:89–91, 1933. 2, 4
- [28] Kaiyi Huang, Kaiyue Sun, Enze Xie, Zhenguo Li, and Xihui Liu. T2i-compbench: A comprehensive benchmark for open-world compositional text-to-image generation, 2023. 2
- [29] Michael Saxon and William Yang Wang. Multilingual conceptual coverage in text-to-image models. In Anna Rogers, Jordan Boyd-Graber, and Naoaki Okazaki, editors, *Proceedings of the 61st Annual Meeting of the Association for Computational Linguistics (Volume 1: Long Papers)*, pages 4831–4848, Toronto, Canada, July 2023. Association for Computational Linguistics. doi: 10.18653/v1/2023.acl-long.266. URL <https://aclanthology.org/2023.acl-long.266>. 2
- [30] Michael Saxon, Yiran Luo, Sharon Levy, Chitta Baral, Yezhou Yang, and William Yang Wang. Lost in translation? translation errors and challenges for fair assessment of text-to-image models on multilingual concepts. *arXiv preprint arXiv:2403.11092*, 2024. 2
- [31] Federico Bianchi, Pratyusha Kalluri, Esin Durmus, Faisal Ladhak, Myra Cheng, Debora Nozza, Tatsunori Hashimoto, Dan Jurafsky, James Zou, and Aylin Caliskan. Easily Accessible Text-to-Image Generation Amplifies Demographic Stereotypes at Large Scale. In *Proceedings of the 2023 ACM Conference on Fairness, Accountability, and Transparency, FAccT ’23*, pages 1493–1504. Association for Computing Machinery. ISBN 9798400701924. doi: 10.1145/3593013.3594095. URL <https://dl.acm.org/doi/10.1145/3593013.3594095>. 2
- [32] Micah Hodosh, Peter Young, and Julia Hockenmaier. Framing image description as a ranking task: Data, models and evaluation metrics. In Michael Wooldridge and Qiang Yang, editors, *IJCAI 2015 - Proceedings of the 24th International Joint Conference on Artificial Intelligence*, IJCAI International Joint Conference on Artificial Intelligence, pages 4188–4192. International Joint Conferences on Artificial Intelligence, 2015. 24th International Joint Conference on Artificial Intelligence, IJCAI 2015 ; Conference date: 25-07-2015 Through 31-07-2015. 3
- [33] Bryan A. Plummer, Liwei Wang, Chris M. Cervantes, Juan C. Caicedo, Julia Hockenmaier, and Svetlana Lazebnik. Flickr30k entities: Collecting region-to-phrase correspondences for richer image-to-sentence models, 2016. 3
- [34] Xinlei Chen, Hao Fang, Tsung-Yi Lin, Ramakrishna Vedantam, Saurabh Gupta, Piotr Dollar, and C. Lawrence Zitnick. Microsoft coco captions: Data collection and evaluation server, 2015. 3
- [35] Jiahui Yu, Yuanzhong Xu, Jing Yu Koh, Thang Luong, Gunjan Baid, Zirui Wang, Vijay Vasudevan, Alexander Ku, Yinfei Yang, Burcu Karagol Ayan, et al. Scaling autoregressive models for content-rich text-to-image generation. *arXiv preprint arXiv:2206.10789*, 2(3):5, 2022. 3, 6
- [36] Jaemin Cho, Abhay Zala, and Mohit Bansal. Dall-eval: Probing the reasoning skills and social biases of text-to-image generation models, 2023. 3
- [37] Yuval Kirstain, Adam Polyak, Uriel Singer, Shahbuland Matiana, Joe Penna, and Omer Levy. Pick-a-pic: An open dataset of user preferences for text-to-image generation. *Advances in Neural Information Processing Systems*, 36, 2024. 3
- [38] Michal Yarom, Yonatan Bitton, Soravit Changpinyo, Roei Aharoni, Jonathan Herzig, Oran Lang, Eran Ofek, and Idan Szpektor. What you see is what you read? improving text-image alignment evaluation, 2023. 3

- [39] John W Pratt, Jean D Gibbons, John W Pratt, and Jean D Gibbons. Kolmogorov-smirnov two-sample tests. *Concepts of nonparametric theory*, pages 318–344, 1981. 4
- [40] Vance W Berger and YanYan Zhou. Kolmogorov–smirnov test: Overview. *Wiley statsref: Statistics reference online*, 2014. 4
- [41] Alec Radford, Jong Wook Kim, Chris Hallacy, Aditya Ramesh, Gabriel Goh, Sandhini Agarwal, Girish Sastry, Amanda Askell, Pamela Mishkin, Jack Clark, et al. Learning transferable visual models from natural language supervision. In *International conference on machine learning*, pages 8748–8763. PMLR, 2021. 5, 6
- [42] Dustin Podell, Zion English, Kyle Lacey, Andreas Blattmann, Tim Dockhorn, Jonas Müller, Joe Penna, and Robin Rombach. Sdxl: Improving latent diffusion models for high-resolution image synthesis, 2023. 6
- [43] Tsung-Yi Lin, Michael Maire, Serge Belongie, James Hays, Pietro Perona, Deva Ramanan, Piotr Dollár, and C Lawrence Zitnick. Microsoft coco: Common objects in context. In *Computer Vision—ECCV 2014: 13th European Conference, Zurich, Switzerland, September 6-12, 2014, Proceedings, Part V 13*, pages 740–755. Springer, 2014. 6
- [44] Yuheng Zha, Yichi Yang, Ruichen Li, and Zhiting Hu. Alignscore: Evaluating factual consistency with a unified alignment function. *arXiv preprint arXiv:2305.16739*, 2023. 6
- [45] Chao Jia, Yinfei Yang, Ye Xia, Yi-Ting Chen, Zarana Parekh, Hieu Pham, Quoc Le, Yun-Hsuan Sung, Zhen Li, and Tom Duerig. Scaling up visual and vision-language representation learning with noisy text supervision. In *International conference on machine learning*, pages 4904–4916. PMLR, 2021. 6
- [46] Chenliang Li, Haiyang Xu, Junfeng Tian, Wei Wang, Ming Yan, Bin Bi, Jiabo Ye, Hehong Chen, Guohai Xu, Zheng Cao, et al. mplug: Effective and efficient vision-language learning by cross-modal skip-connections. *arXiv preprint arXiv:2205.12005*, 2022. 14
- [47] Qinghao Ye, Haiyang Xu, Guohai Xu, Jiabo Ye, Ming Yan, Yiyang Zhou, Junyang Wang, Anwen Hu, Pengcheng Shi, Yaya Shi, Chaoya Jiang, Chenliang Li, Yuanhong Xu, Hehong Chen, Junfeng Tian, Qian Qi, Ji Zhang, and Fei Huang. mplug-owl: Modularization empowers large language models with multimodality, 2023. 14
- [48] Hugo Touvron, Thibaut Lavril, Gautier Izacard, Xavier Martinet, Marie-Anne Lachaux, Timothée Lacroix, Baptiste Rozière, Naman Goyal, Eric Hambro, Faisal Azhar, Aurelien Rodriguez, Armand Joulin, Edouard Grave, and Guillaume Lample. Llama: Open and efficient foundation language models. *arXiv preprint arXiv:2302.13971*, 2023. 14
- [49] Lianmin Zheng, Wei-Lin Chiang, Ying Sheng, Siyuan Zhuang, Zhanghao Wu, Yonghao Zhuang, Zi Lin, Zhuohan Li, Dacheng Li, Eric P Xing, Hao Zhang, Joseph E. Gonzalez, and Ion Stoica. Judging llm-as-a-judge with mt-bench and chatbot arena, 2023. 14
- [50] Haotian Liu, Chunyuan Li, Qingyang Wu, and Yong Jae Lee. Visual instruction tuning, 2023. 14
- [51] Haotian Liu, Chunyuan Li, Yuheng Li, and Yong Jae Lee. Improved baselines with visual instruction tuning, 2023. 14
- [52] Junnan Li, Dongxu Li, Caiming Xiong, and Steven Hoi. Blip: Bootstrapping language-image pre-training for unified vision-language understanding and generation. In *ICML*, 2022. 14
- [53] Wenliang Dai, Junnan Li, Dongxu Li, Anthony Meng Huat Tiong, Junqi Zhao, Weisheng Wang, Boyang Li, Pascale Fung, and Steven Hoi. Instructblip: Towards general-purpose vision-language models with instruction tuning, 2023. 14
- [54] Rohan Bavishi, Erich Elsen, Curtis Hawthorne, Maxwell Nye, Augustus Odena, Arushi Somani, and Sağnak Taşlılar. Introducing our multimodal models (fuyu-8b), 2023. URL <https://www.adept.ai/blog/fuyu-8b>. 14
- [55] Josh Achiam, Steven Adler, Sandhini Agarwal, Lama Ahmad, Ilge Akkaya, Florencia Leoni Aleman, Diogo Almeida, Janko Altenschmidt, Sam Altman, Shyamal Anadkat, et al. Gpt-4 technical report. *arXiv preprint arXiv:2303.08774*, 2023. 14
- [56] Jared Kaplan, Sam McCandlish, Tom Henighan, Tom B Brown, Benjamin Chess, Rewon Child, Scott Gray, Alec Radford, Jeffrey Wu, and Dario Amodei. Scaling laws for neural language models. *arXiv preprint arXiv:2001.08361*, 2020. 15

- [57] Avijit Thawani, Jay Pujara, and Filip Ilievski. Numeracy enhances the literacy of language models. In Marie-Francine Moens, Xuanjing Huang, Lucia Specia, and Scott Wen-tau Yih, editors, *Proceedings of the 2021 Conference on Empirical Methods in Natural Language Processing*, pages 6960–6967, Online and Punta Cana, Dominican Republic, November 2021. Association for Computational Linguistics. doi: 10.18653/v1/2021.emnlp-main.557. URL <https://aclanthology.org/2021.emnlp-main.557>. 21
- [58] Dominic Petrak, Nafise Sadat Moosavi, and Iryna Gurevych. Improving the numerical reasoning skills of pretrained language models. *arXiv preprint arXiv:2205.06733*, 2022. 21
- [59] Karthik Valmeekam, Alberto Olmo, Sarath Sreedharan, and Subbarao Kambhampati. Large language models still can’t plan (a benchmark for llms on planning and reasoning about change). *arXiv preprint arXiv:2206.10498*, 2022. 21
- [60] Subbarao Kambhampati, Karthik Valmeekam, Lin Guan, Kaya Stechly, Mudit Verma, Siddhant Bhambri, Lucas Saldyt, and Anil Murthy. Llms can’t plan, but can help planning in llm-modulo frameworks. *arXiv preprint arXiv:2402.01817*, 2024. 21

A Supplementary Details

A.1 Equations for evaluated metrics

Embedding correlation metrics CLIPScore and ALIGNScore are computed using positive cosine similarity between text and image features, from feature extractor model \mathcal{M} as:

$$\text{clip-s}(p, i) = \max(\cos(\mathcal{M}_I(i), \mathcal{M}_T(p)), 0) \tag{6}$$

VQA metrics VLM-VQA metrics like TIFA and DSG are assessed by a multiple choice question assessment model (\mathcal{M}_B and a vision-language model \mathcal{M}_{VL} over questions Q generated by an LLM based on the prompt p .

$$\text{tifa-s}(p, i) = \frac{1}{|Q|} \sum_{(q,a) \in Q} \mathbb{1}(\mathcal{M}_B(\mathcal{M}_{VL}(i, q)) = a) \tag{7}$$

A.2 VLM details

mPLUG is a class of vision-language models that use skip connections between visual encoder embedding layers between cross-modal attention blocks in the transformer stack [46]. We use the mPLUG-OWL [47] 7b checkpoint which uses LLaMA 7b [48] as the pretrained text encoder.

LLaVA is a fine-tune of Vicuna [49] (decoder-only transformer model) that uses a learned MLP “vision-language connector” layer to map a single input image’s CLIP encodings into a shared embedding space [50, 51]. We use LLaVA 1.5 13b. Because LLaVA was instruction fine-tuned for chat applications, we experiment with a variant system prompt that requests *concise* answers from the system. We mark this alternate option LLaVa 1.5 (alt) in plots and figures.

BLIP is a jointly-trained self-attention ViT trained with cross attention to multiple transformer encoder and decoder pipelines with different tasks [52]. We use the BLIP encoder/causal LM decoder combination as a transformer encoder-decoder model to produce VQA answers from the `blip-vqa-base` checkpoint.

InstructBLIP extends BLIP by including an instruction fine-tuned “Q-Former” that selects salient instruction-related visual features from a frozen ViT for input to a frozen LLM that answers the query conditioned on the selected features [53]. We use `instructblip-flan-t5-xl`.

Fuyu is a decoder-only VLM that splits an input image into a sequence of patches that are separately projected directly into the transformer embedding space, which jointly learns ViT and LM behaviors [54]. We use `Fuyu-8b`.

GPT4-V is the largest state-of-the-art VLM provided by OpenAI [55]. It is expensive to run!

A.3 Compute cost estimates

Estimating FLOPs per inference pass for each model. We use OpenAI’s estimate [56] of $\approx 2N$ OPs per forward pass for a large transformer model, where N is the total number of parameters.

Obtaining parameter count estimates for closed models. TIFA, DSG, and LLMscore use some combination of GPT3 and GPT4, whose exact parameter counts and FLOP/inference costs haven’t been publicly disclosed. We use [estimates from SemiAnalysis](#) to get an approximate FLOP cost. While these numbers are likely imperfect, their orders of magnitude are as accurate as we can get.

Obtaining metric FLOP cost per single image eval. Given FLOP/forward pass estimates for each model, our estimates of the FLOP cost to evaluate an image is a function of the number of model calls and estimated tokens per call. The embedding-correlation metrics require 2 calls to an embedding model, matmul and sum operations to get the cosine similarity. TIFA requires on average 8 questions, with GPT-3 question-generating calls of average 40 tokens, and VQA model calls of average length 20 tokens. For DSG these numbers are 5, 40, 15. The costs of calling the freeform-to-multiple choice model are negligible. We estimate that LLMscore and VIEScore both require approximately 50 tokens of LLM or VLM compute to score an image. LLMscore’s use of mPLUG to caption is negligible alongside the cost of running GPT-3.

Total compute cost of our study. In total, we estimate our study took 9.89×10^{18} FLOPs, mostly through OpenAI’s service, but also on lab-owned NVIDIA Titan-X and A-100 GPUs.

A.4 Semantic Error Graph Structure

For more information on the structure of the semantic error graphs (SEGs), we provide examples here. SEG 85 is one example with a more interesting topology than the example in Figure 1. Figure 5 has a structure including two-error edges, single-parent nodes, single-child nodes, multi-parent nodes, and multi-child nodes in the same graph, corresponding to prompt “*guy with umbrella hat sitting at a table with another person with a hat under a red umbrella.*”

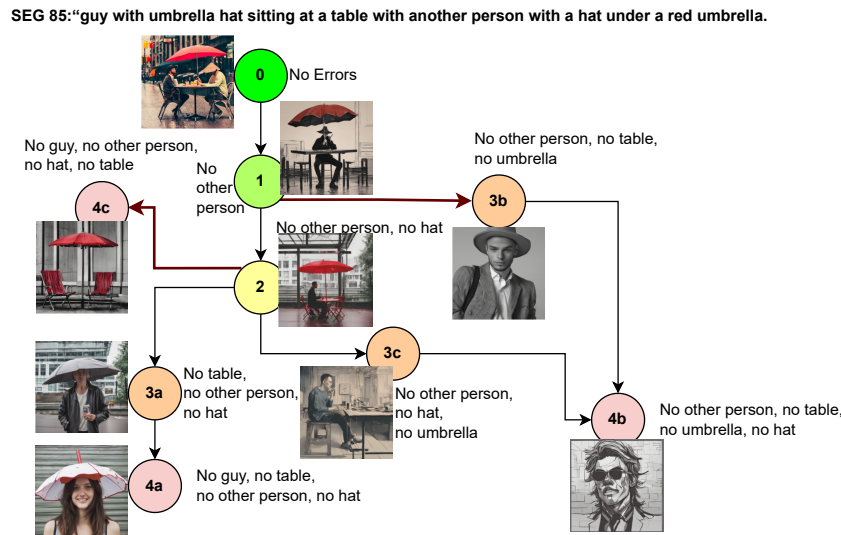


Figure 5: Example of a SEG (85) with a more complex structure. Some nodes have multiple child nodes, and some edges correspond to more than one error (dark red).

SEG 109: a Mesoamerican pyramid surrounded by jungle. Detailed charcoal sketch.

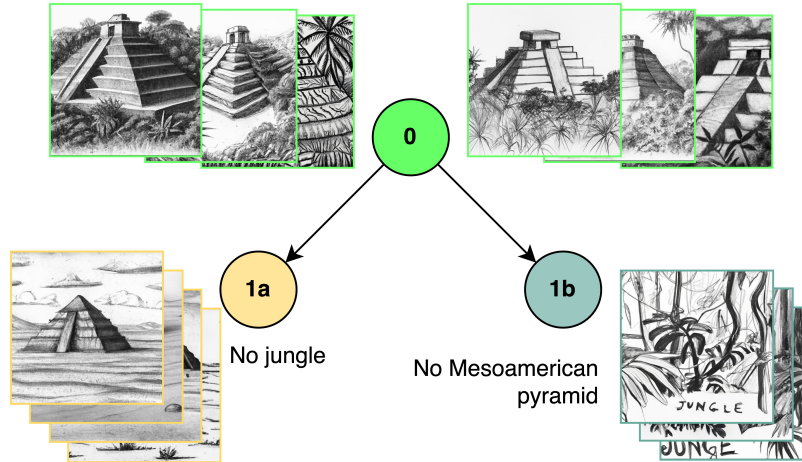


Figure 6: Example of a SEG (109) with a simpler structure. We show multiple images for each of the three nodes in this SEG.

A.5 Scoring within SEGs

Figure 7 exemplifies why we choose to only score rank order *along walks* of the graph, rather than *between all pairs of nodes*. A priori there’s no reason the beach-less images should be worse than the umbrellas, yet metrics consistently rate the beach error more severe.

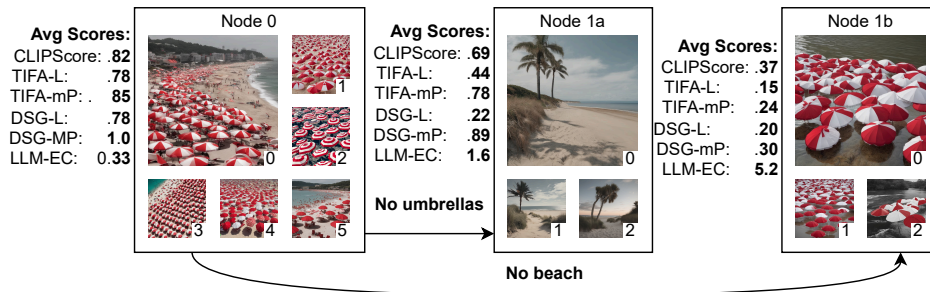


Figure 7: Examples from SEG 71 (*The beach is crowded with red and white umbrellas*). Even though both nodes 1a and 1b have the same error count (1) they systematically differ across all metrics: all metrics punish the images where the umbrellas are just in water (no beach, 1b) more than they penalize an empty beach with no umbrellas (1a).

B Supplementary Results

B.1 Comparing DSG question evaluation using DSG and TIFA score accumulation methods

The first few steps of TIFA [16] and Davidsonian Scene Graph (DSG) [6] scoring methods are nearly identical: an LLM generates a set of requirements as questions, and a VQA system answers them. However, the two methods differ chiefly in how the answers are combined into a single image-level score. TIFA simply scores images by the correct answer rate, while DSG uses the graph structure of the requirements to build in some robustness: if an *upstream* requirement is not met (e.g., *is there a boy?* : **no**), then *downstream* requirements are all also assessed as not being met, regardless of answer. In the example provided, if the question “*is the boy’s shirt green?*” were answered **yes**, the DSG accumulation technique would still score this requirement as being not met, due to the upstream requirement, while the TIFA accumulation method would score it as being met.

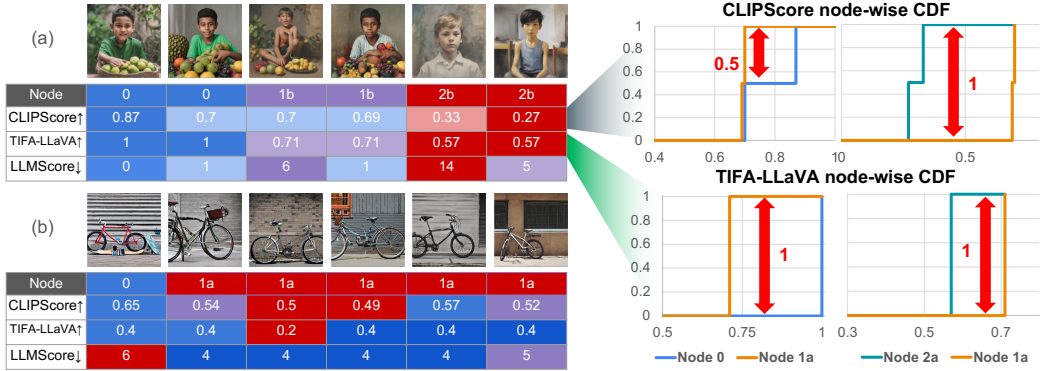


Figure 8: Examples of scores assigned by three metrics to examples from an easy (a) and hard (b) semantic error graph (left). Computation of the separation score $\text{sep}_m(S)$ for two metrics is depicted at the right. Color coding of each cell corresponds to the metric’s score for the image being better (blue) or worse (red); more correlated measures (presenting a higher rank order score $\text{rank}_m(S)$) will show the same progression from red to blue (a), while harder-to-rank examples will not (b).

		<i>mPLUG</i>	<i>LLaVA 1.5</i>	<i>LLaVA 1.5 (alt)</i>	<i>InstructBLIP</i>	<i>BLIP1</i>	<i>Fuyu</i>										
		DSG w/ TIFA accumulation						DSG w/ DSG accumulation									
Ord.	Avg	70.4	76.2	75	79.0	76.6	29.5	68.8	80.0	75.6	80.2	76.9	35.8				
	Synth	74.6	80.1	81.6	85.1	81.6	35.4	73.5	83.8	82.1	86.1	81.7	45.5				
	Nat	65.3	65.9	68.8	<i>70.7</i>	71.6	20.5	61.9	74.9	68.9	70.2	71	21.5				
	Real	58.4	70.0	54.2	62	61.2	14.2	56.4	69.6	55.9	65.8	62.8	10				
Sep.	Avg	78.4	83.1	80.3	84.2	80.8	63.6	75.5	82.5	80.5	84.3	80.6	66				
	Synth	80.9	85.7	83.9	87.8	84.9	65.8	77.1	85.5	83.8	88.8	84.1	68.7				
	Nat	71.2	80.9	76.7	81.8	73.3	68.6	70.6	75.1	77.2	81.5	75.1	71				
	Real	75.1	74.5	69.4	71.9	70.8	50.3	73.1	76.8	70.6	68.9	71.4	50.8				

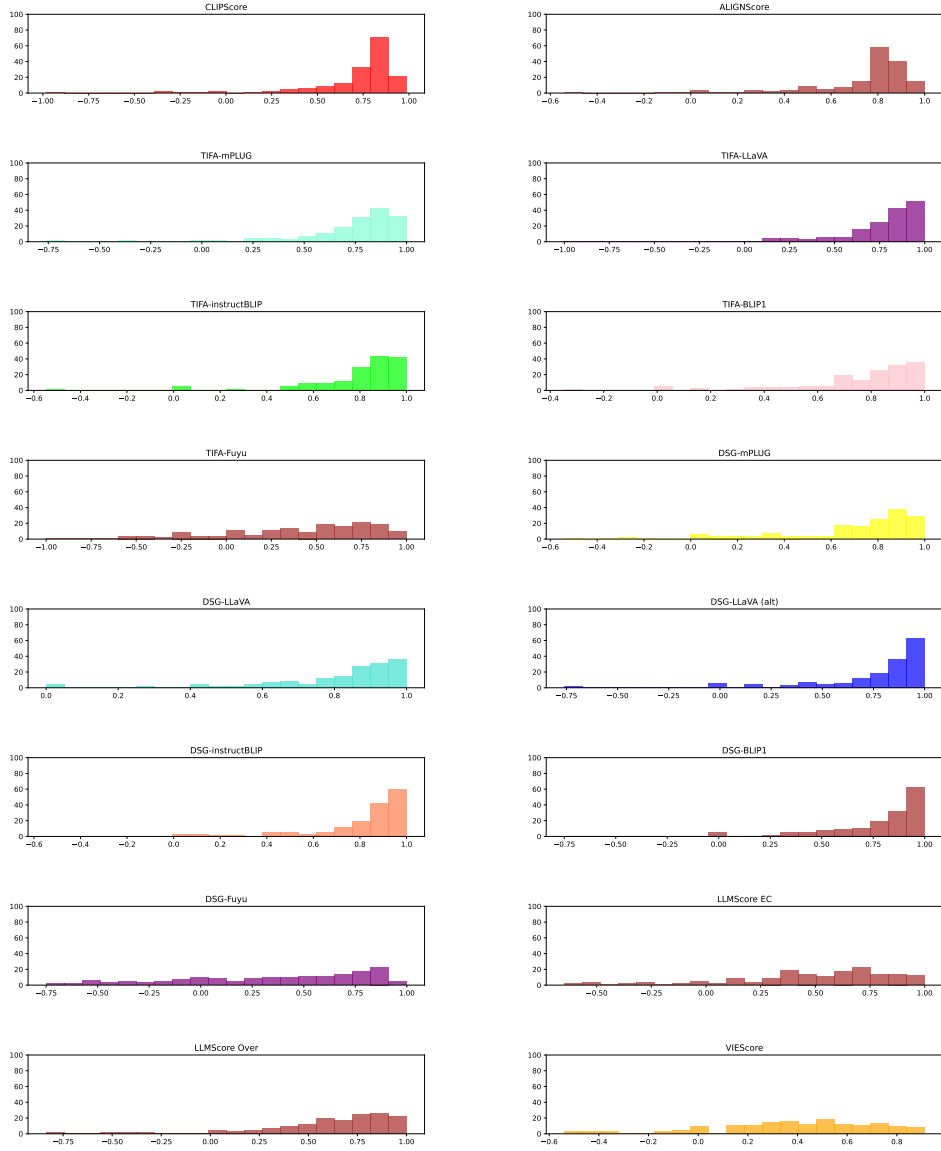
Table 3: Comparing how using DSG vs TIFA-style accumulation for scoring each image by DSG questions impacts performance along both our metrics. The right half of this table is identical to the DSG section in Table 2, and bold, italic, and highlighting follows the same rules, except cells in the TIFA half are marked as if they were replacing the right half cells in the DSG section in Table 2.

As a supplementary experiment, we compare how accumulating the DSG questions using the DSG technique compares to accumulating them with the TIFA technique in Table 3. Interestingly, the impact of this change differs between strong and weak VLMs, between ordering and separation scores, and between the easier and harder subsets. For example, switching from the DSG to TIFAstyle accumulation consistently *improves ordering performance for mPLUG*, while it *worsens performance for LLaVA, InstructBLIP, and BLIP1*. For Fuyu, the weakest model, DSGstyle accumulation *significantly improves performance* over TIFA. This strengthens the claim from [6] that using the scene graph to check requirements adds robustness; it makes a lot of sense that this robustness benefits the lowest-performing VQA systems the most.

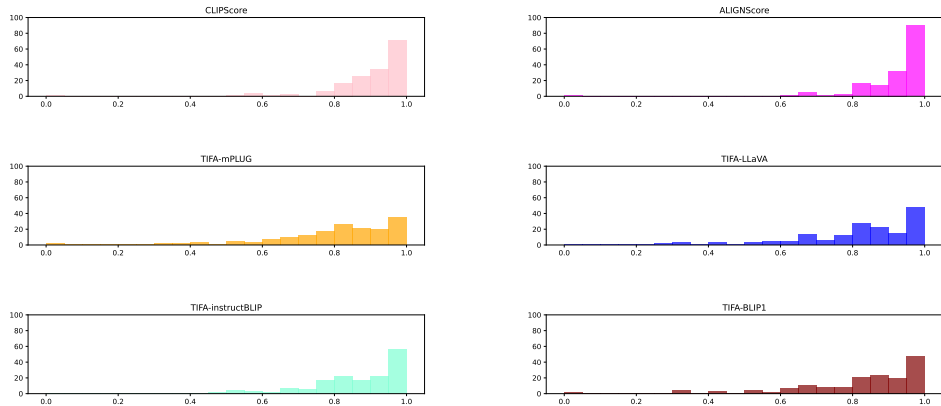
For separation scores, TIFA accumulation improves performance of more models. In particular, TIFA accumulation pushes InstructBLIP into the top 3 for separation on the Synth subset, while no DSG metric using DSG accumulation breaks into the top 3 (red highlighted cell).

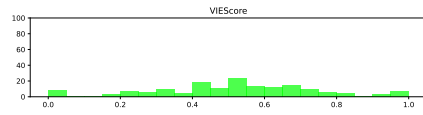
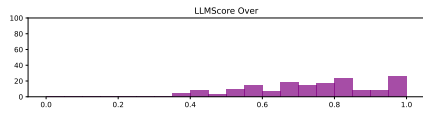
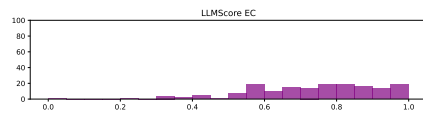
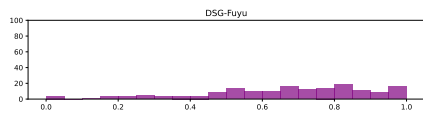
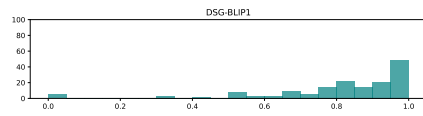
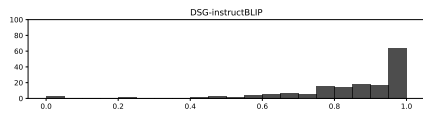
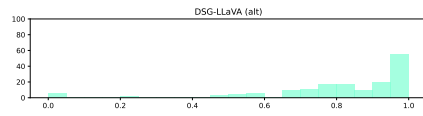
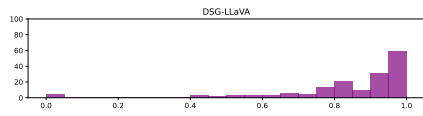
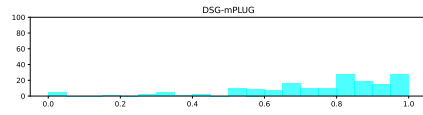
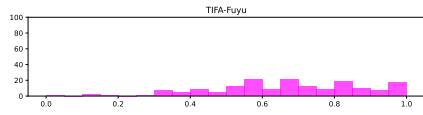
B.2 Modelwise Spearman Ordering Score Histograms

Here we provide full histograms for our Spearman Ordering and Kolmogorov–Smirnov Separation scores, across every SEG, for all metrics we assessed.

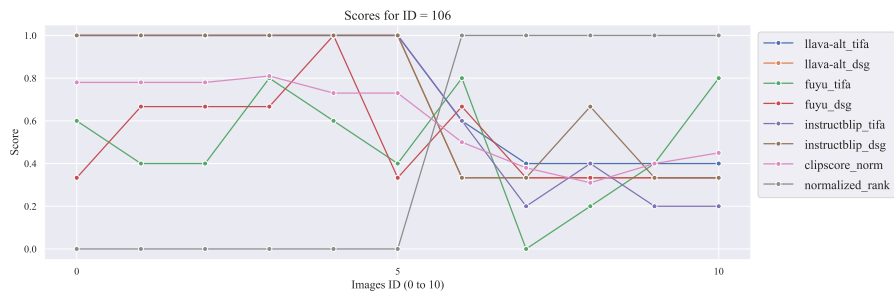
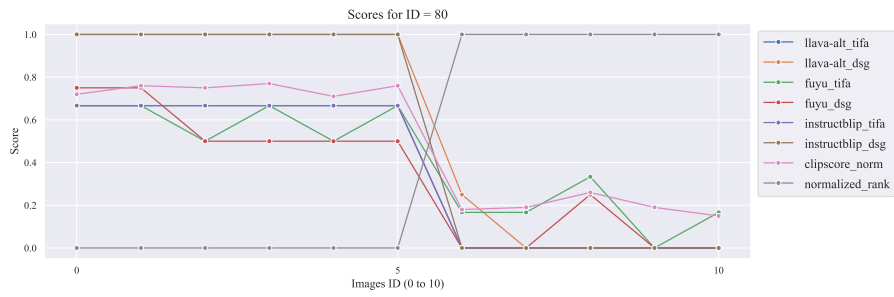
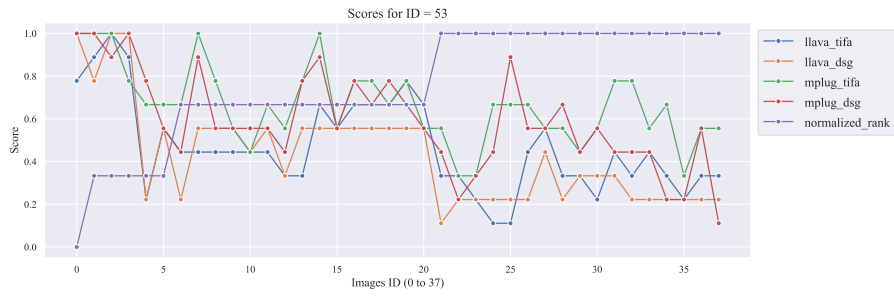
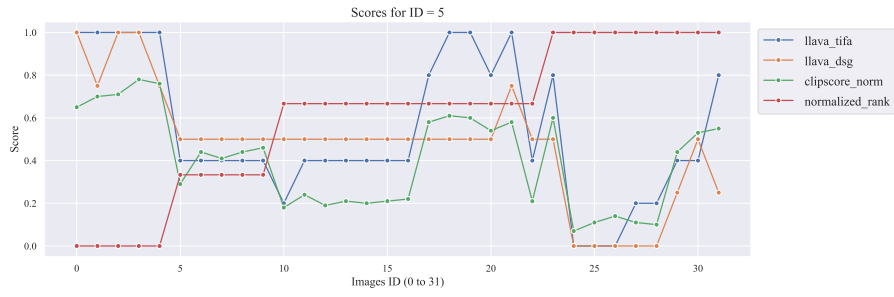


B.3 Modelwise K-S Separation Score Histograms





Here we provide line plots for a set of metrics and SEGs. Note that for `normalized_rank`, higher is worse (more errors). High-correlation is assessed when the metric lines (higher better) go down as the metric lines (higher better) go up.



C Supplementary Analysis

Another interesting weakness of the QG/A metrics is that many unlucky situations where the VLM backend presents a mix of true and false positives that cause incorrect rankings or poor separation (DSG fails to order samples while CLIPScore succeeds in fig. 9) to occur. However, these VLM failures cases are interpretable and can be targeted; **T2IScoreScore** will hopefully drive future work in making LMs more robust to these sorts of errors for VQA to mitigate this issue. In addition to these interpretability advantages, the more sophisticated VLM-based metrics still do present better subjective human preference correlation than CLIPScore [6, 16–18]. By focusing exclusively on objective similar-image ordering and separation, **TS2** is effectively orthogonal to these preference evals.

Given the documented biases LLMs have in directly outputting numbers [57, 58], it isn't a surprise that the technique which directly prompts VLMs to output a numerical preference value (VIEScore) is at present the least robust.

In general it seems that the most successful methods that leverage VLMs (TIFA and DSG) still ultimately produce scores using a deterministic algorithm. They use VLMs in a perceptual manner to separately check each requirement, but the final score is the accuracy estimate from each separate VQA question. This comports with the theories of LLM function that treat it as a “system 1” [59]; effectively TIFA and DSG are examples of *VLM-modulo* frameworks outperforming pure LLMs on the task of prompt coherence scoring [60].

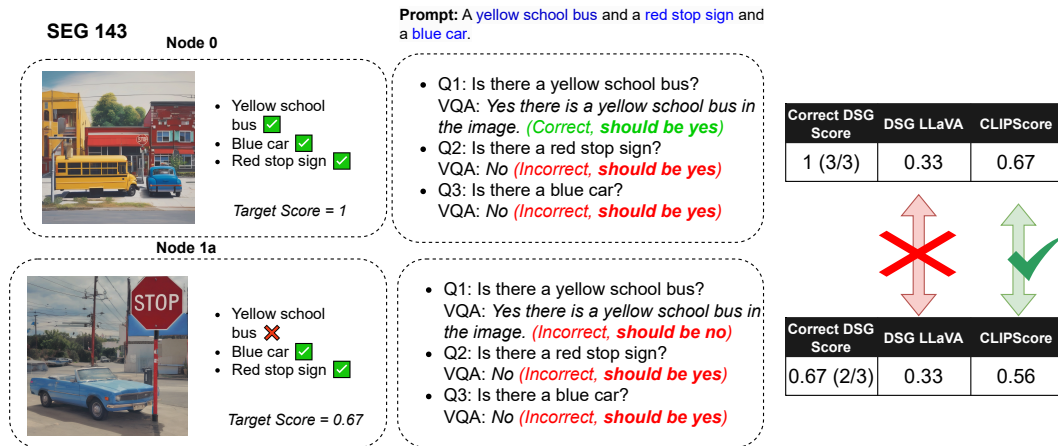


Figure 9: Example of two images on nodes 0 and 1 from a hard SEG that are correctly separated (and ranked) by CLIPScore but are not separated by DSG-LLaVA. VLM hallucinations are a key hinderance to QG/A performance on **TS2**.

Are the same SEGs hard for the same models? fig. 10 and fig. 11 present correlation plots between SEG-wise rank_m and sep_m scores respectively between each pair of metrics. For both we show (a) the correlations over all SEGs, and (b) the correlations between only SEGs in the Real subset. These plots show that broadly, similar methods have similar “blind spot” SEGs, while different ones can vary wildly in terms of which examples they succeed and fail at ordering and separating. Note that all TIFA or DSG QG/A metrics have appreciable correlation to each other, provided they use a strong enough VLM. The metrics employing weak VLMs such as Fuyu do not perform well. Similarly, the two LLMscore metrics are highly correlated to each other; the pure VLM numerical rating methods are not producing random noise. These correlations are stronger in the full set of SEGs (including natural images and the easy, pre-designed Synth SEGs) than they are in the hardest Real set of SEGs.

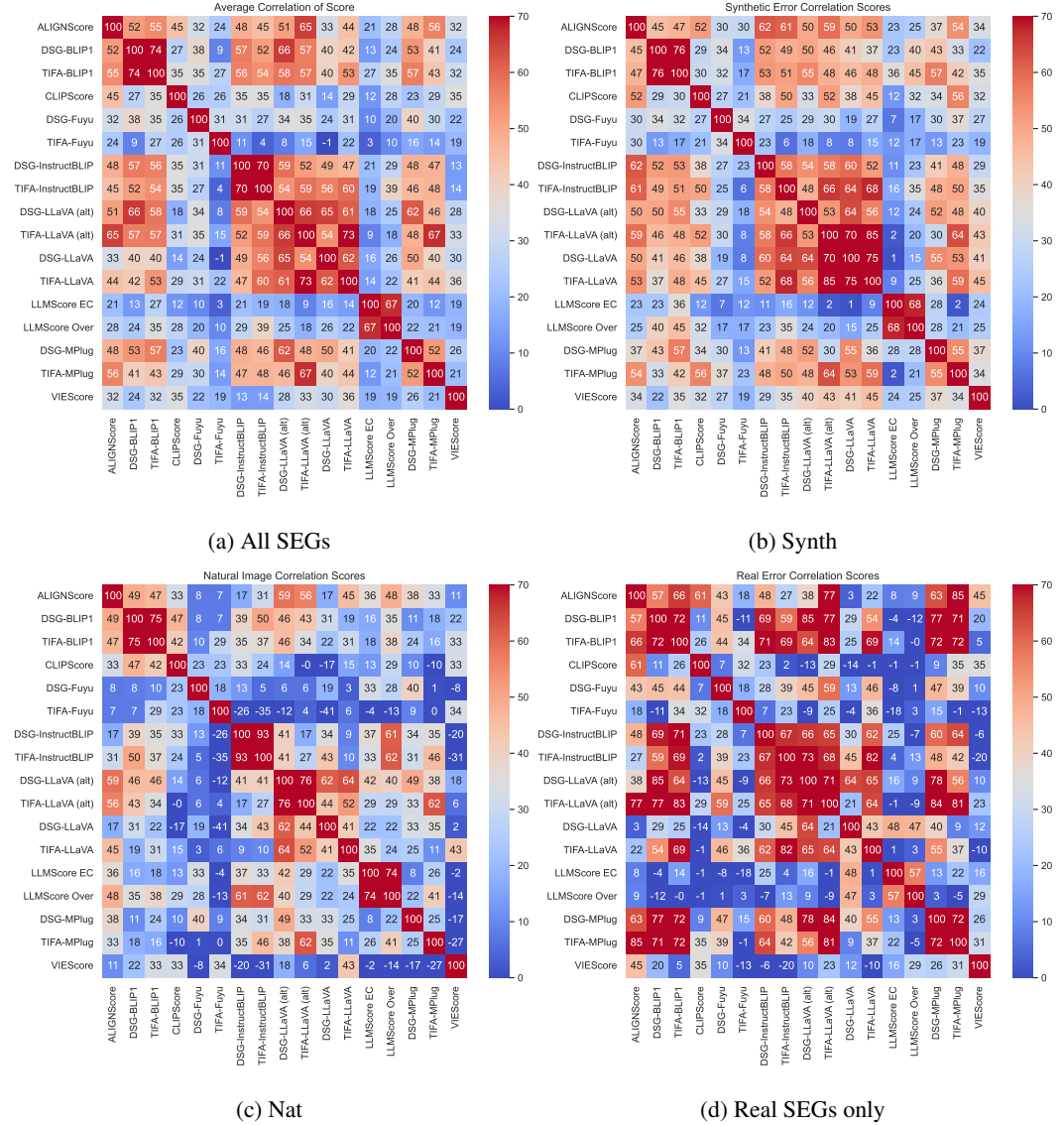


Figure 10: Correlation between the Spearman correlation score for each prompt tree for each metric, for all SEGs (a), for the synthetic error SEGs (b), for the natural image/synthetic error SEGs (c) and for the real error subset (d).

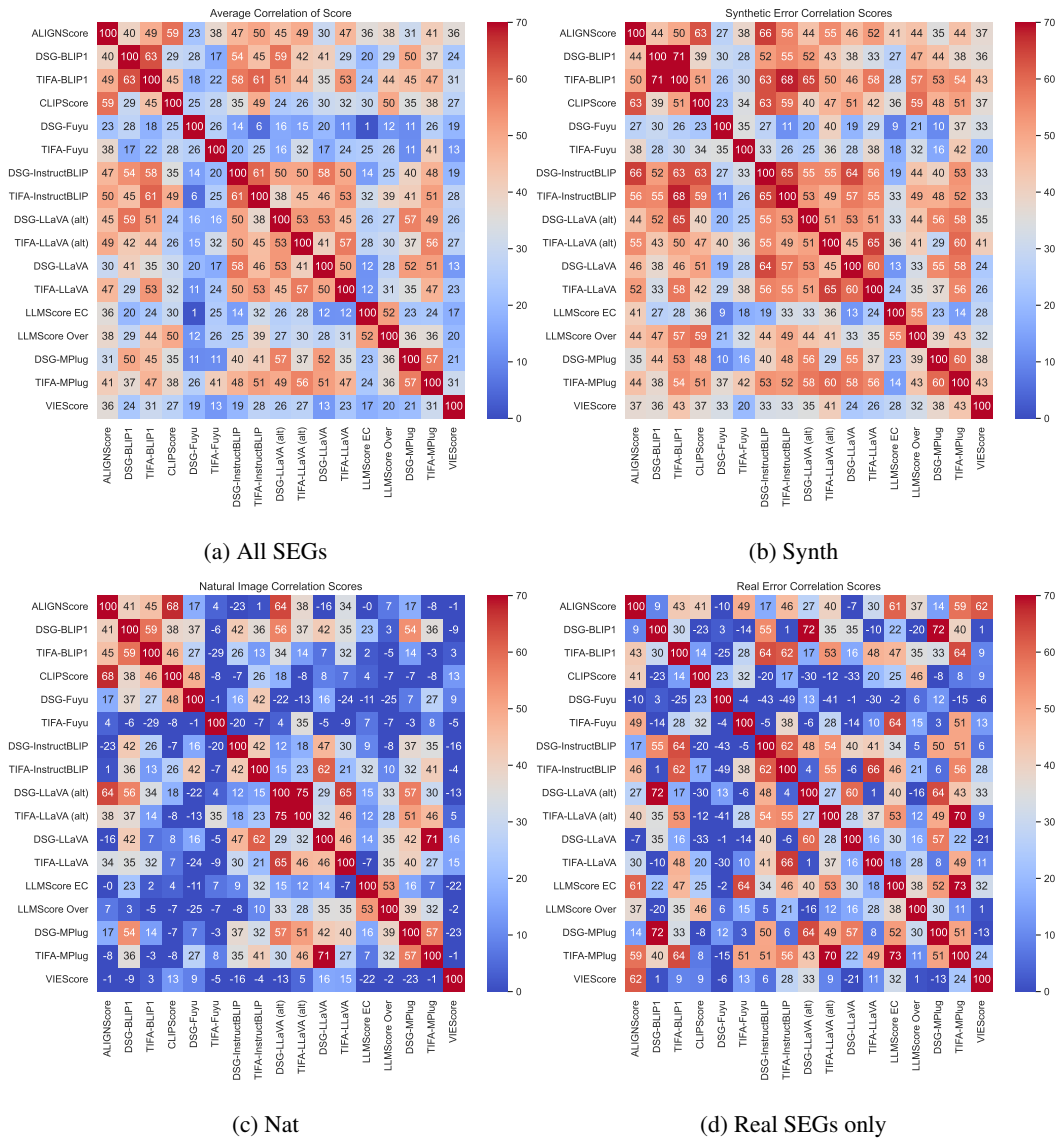


Figure 11: Correlation between the K-S Separation score for each prompt tree for each metric, for all SEGs (a), for the synthetic error SEGs (b), for the natural image/synthetic error SEGs (c) and for the real error subset (d).

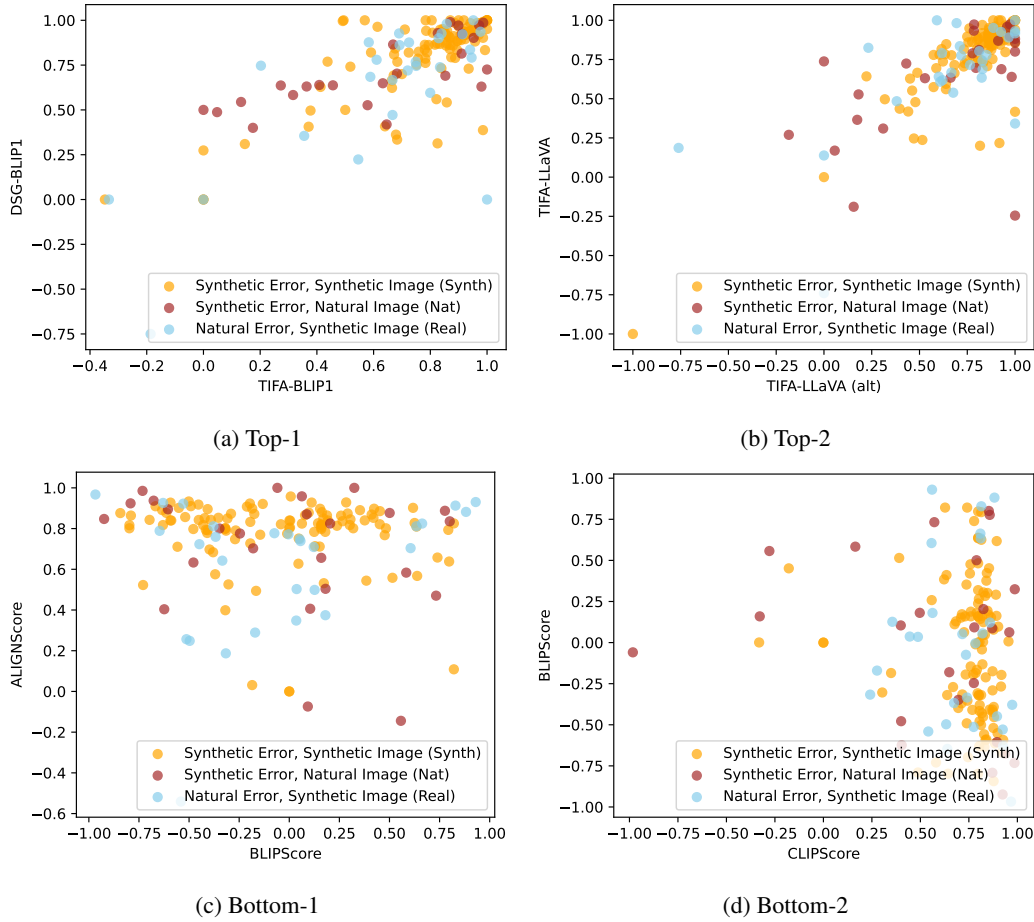


Figure 12: Scatter plots comparing the two most correlated metrics (a, b) by Spearman correlation Ordering score across the Synth, Nat, and Real populations, and the two least-correlated (c, d). Note that the two highest-correlated metrics are both QG/A metrics using the same underlying VLM (DSG and TIFA using BLIP1, (a); TIFA using LLaVA with two different system prompts, (b)).

Figure 12 and Figure 13 show scatter plots for the Ordering (Spearman) and Separation (KS statistic) scores for every SEG between the most highly-correlated (a, b) and low-correlation (c, d) pairs of metrics under evaluation, respectively.

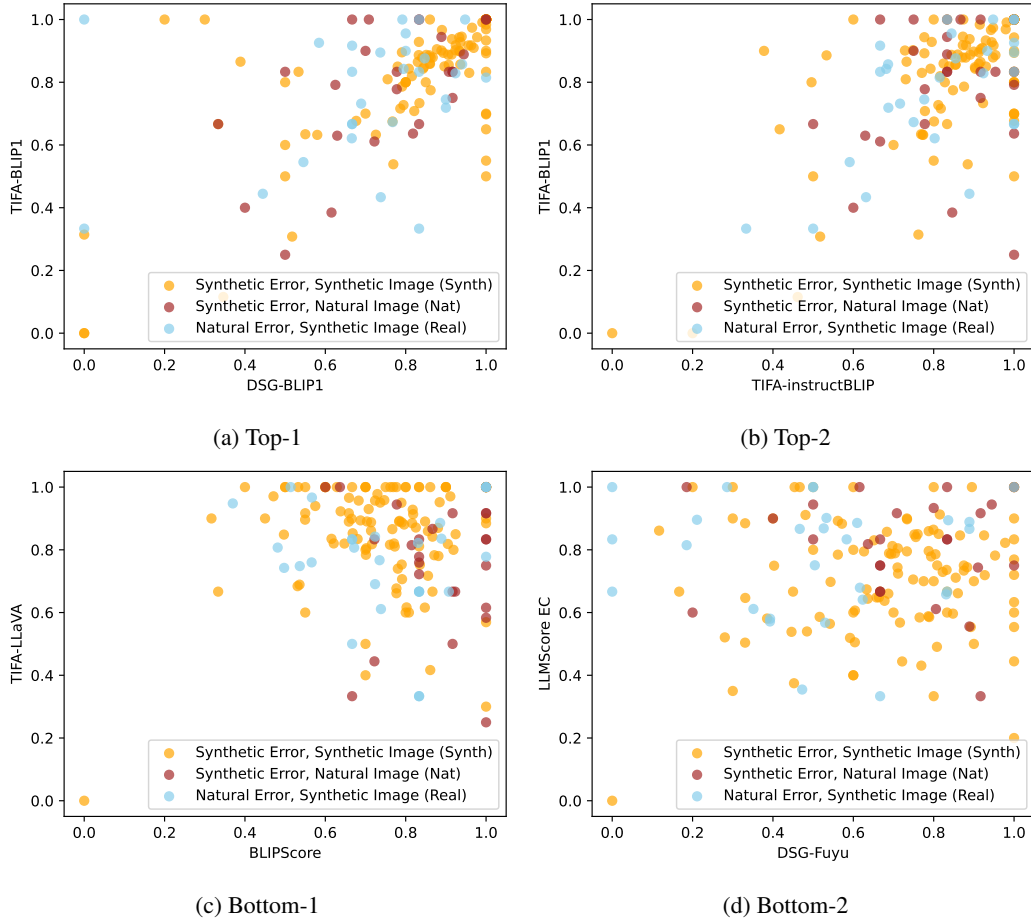


Figure 13: Scatter plots comparing the two most correlated metrics (a, b) by Kolmogorov–Smirnov Separation score across the Synth, Nat, and Real populations, and the two least-correlated (c, d). Note that the two highest-correlated metrics are both QG/A metrics using the same or related underlying VLMs (DSG and TIFA using BLIP1, (a); TIFA using BLIP1 and InstructBLIP, (b)).

Both of these sets of figures confirm that similar underlying VLMs by-and-large “think” similarly in terms of scoring models, even over different sets of questions (TIFA and DSG). This suggests that development of overall better VLMs will generalize to many different types of VLM evaluations.